Grating-Lobe Reduction for Non-Uniform Linear Sub-Array Using High Order Mode

M. Etebarian Khorasgani   Department of Electrical Engineering; Amirkabir University of Technology (Tehran Polytechnic); Tehran, Iran; Email: m.etebarian1997@gmail.com

A. Ghorbani*   [Corresponding Author] Department of Electrical Engineering; Amirkabir University of Technology (Tehran Polytechnic); Tehran, Iran; Email: ghorbani@aut.ac.ir

Abstract: In antenna theory, a sub-array is a group of smaller antennas arranged into an array. It is a collection of smaller elements in the structure of an array antenna. Not only does this structure have advantages for performance antennas, but also the sub-array has problems, such as the occurrence of grating lobes (GLs) in the radiation pattern. Some of the advantages of these structures are reduced complexity, cost efficiency, and system flexibility. GLs are unwanted patterns that occur when the spacing between antenna elements is large relative to the signal wavelength. These lobes can appear in undesirable directions, decreasing the antenna's performance, including its directivity and gain. There are several methods for GL reduction, including reducing element spacing, using non-uniform or random spacing to disrupt periodicity, applying beamforming weights to suppress sidelobes, and employing multi-subarray techniques for additional control. The main approach to reducing GLs is to introduce a null in the radiation pattern using the high-order mode technique. This means that when the element pattern is a multiple of the array pattern, the GL is omitted from the pattern at -40 degrees. It is possible to change the radiation direction of an antenna by combining two modes. In other words, the beam scan in the element depends on the current excitation mode. Thus, each mode is excited by a coaxial cable, and each antenna element has two power supplies. Simulation results show that the reduction of GL is -21.54 dB.

Index Terms: Grating Lobe Reduction, Subarray Antenna, High Order Mode.

Journal of Communication Engineering (JCE)

Etebarian Khorasgani & Ghorbani | Grating-Lobe Reduction for Non-Uniform Linear ...

I. INTRODUCTION

The subarray antennas,grouping radiating subunit elements, are a particular component in phased array systems. These structures in an array antenna consist of a collection of element antennas into a subarray that are organized by an independent beamforming network[1], [2], [3]. There are different methods that can be used to design these structures, such as uniform subarrays[4], [5] non-uniform subarrays[6], [7], and overlapped subarrays. A uniform subarray antenna is a type of phased array antenna where a larger array is divided into smaller, identical groups of antenna elements called subarrays. As a result, their elements are spaced equally and have the same signal amplitude and phase relationship.This approach is the opposite of a nonuniform subarray because it is used to overcome the limitations of uniform arrays, especially for large-scale systems. Due to the advantages of subarray antennas, researchers like to design a type of antenna. Subarrays offer important advantages, including reduced complexity, cost efficiency, scalability, and improved beam agility. Phased-MIMO radars are a combined system of MIMO and phased-array radars. Some of the differences between MIMO radar and phased array are enhanced parameter estimation, reduced false alarms, and improved detection performance[8]. Large arrays are used due to their advantages; as a result, the benefits are high gain, high resolution, and strong beam control capability[9]. Zang and his coworker designed a new approach that achieves multibeam antenna gain flatness using reconfigurable subarrays. Phase tuning internally enables different scanning angles, with performance optimized for less gain ripple, significantly improving 2.4 dB and 2.9 dB in the prototype[10]. One of the important phenomena in an antenna array is the presence of a GL in the visible region of the pattern. Although this type of antenna has an advantage, there is an important problem that is the GL. Not only does this phenomenon reduce the directivity of the antenna at a target angle, but also it decreases the signal-to-noise ratio in the receive link. To reduce the GL in the visible region, methods such as using non-uniform elements, non-uniform weighting of array elements, and non-uniform positioning of elements are used. In [11] Yang and his coworker were able to reduce the GL level below −15.9 dB. Metasurface antennas offer hardware advantages but face challenges due to metamaterial elements, causing GLs. A waveguide feed layer mitigates these issues, maintaining cost and manufacturability benefits. This research [12] pays attention analytically to the radiation behavior of a 2D metasurface antenna array formed by tiling 1D waveguide-fed metasurfaces. Another methods [13] are a combination of subarray amplitude weights, random subarray, and row displacement, which reduces GLs in phased array scanning. The staggering technique is simpler and cost-effective. Therefore, a combination is necessary for optimal sidelobe level (SLL) and GL ratios. When using the combined approach proposed in this paper, the simulated results show that the GL

is -20 dB. Zhang and his coworkers have designed an antenna element using the TM_{50} mode,and their suggested methods are proposed to suppress GLs. The GLs level in this research at 22.3GHz is only -22dB[14]. Using a dual-mode circular patch antenna, the GL is suppressed. As a result,we can achieve over 25dB reduction for scan angles up to ±45°[15].The novel approach of this [16] utilizes GL reduction with optimization in planar antenna arrays ,so the spacing between elements is taken into account for a particular lattice. As observed, the structure of elements affects the suppression GL, and an optimum element savings of about 25.03% for 26° elevations is achieved with a triangular array. Recently, one of the excellent topics in modern antennas is high-order modes in advanced antennas. Higher-order mode refers to a specific pattern of electromagnetic field distribution on the antenna structure. Thus, each mode exhibits a unique current distribution and consequently radiates with a distinct radiation pattern. When the GL appears in the radiation pattern at theta degrees, adding a null at the GL angle decreases the magnitude of the GL,and this technique is important in this article[17], [18], [19], [20]. In this paper presents the reduction of GLs by a high-order mode antenna. The structure of this antenna consists of 20 elements, and each element in the array is a ring microstrip patch antenna. Because the array scan beam is at 20 degrees, we should excite the higher-order mode in the element antenna. Due to the total pattern being the multiplication of the array factor and the element pattern, the GL is omitted in the pattern at -40 degrees. The main challenges in designing this type of antenna are using multilayer substrates to excite dual-mode antenna elements, improving the antenna's bandwidth, making the probe position very effective in tuning the amplitude of each mode, and controlling the phase difference between the two modes. This means that the phase difference between the two modes should be 90 degrees so that the direction of radiation can be controlled. Thus, the TM_{11} and TM_{21} are excited in the element antenna , and the GLs are reduced to well below -21.54 dB.

II. ANALYSIS OF GRATING LOBE

One of the important phenomena in an antenna array is the presence of a GL in the visible region of the pattern. Not only does this phenomenon reduce the directivity of the antenna at a target angle, but also it decreases the signal-to-noise ratio in the receive link. In theory, the total electric field from the linear array given by (1) is the sum of the radiation from all elements:

$$AF(\theta) = \sum_{n=1}^{N} I_n e^{j(n-1)\Psi} \tag{1}$$

$$\psi = kd \sin(\theta_O) + \beta = 2m\pi \tag{2}$$

ψ is the total phase difference between adjoining elements. If the phase difference is zero, this function will have maxima lobes in the radiation pattern[21]. For m=0 in the (2) formula, we have a maximum direction at θ_0, which is given by (2). If m is to be greater than one, we can see another maximum lobe in the radiation pattern. Fig. 1(a) shows the geometry of a 20-element circular antenna array with an element spacing of a wavelength. As is shown in Fig. 1(b), by scanning the array elements at an angle of +20 degrees, we can see a maximum lobe in the radiation pattern at an angle of -40°. Therefore, the magnitude of the GL at -40° degrees must be reduced. Therefore, GL is eliminated by creating a null point at an angle of -40 degrees in the antenna radiation pattern.

III. SYNTHESIS NULL IN ELEMENT PATTERN

According to the theory, the general relationship of the antenna pattern is equal to the multiple of a single element and an array factor in (3).

$$P_T = P_E \times P_A \tag{3}$$

Where P_E and P_A are the radiation patterns of the array and the element pattern. Typically, various methods are employed, including element amplitude and phase synthesis, the use of non-uniform elements, and aperture in the array structure. However, another key point often ignored is the element pattern. By adding null to the element pattern, we can achieve GL reduction.

In other words, one of the key parameters that affects the suppression of GL in total pattern antennas is the element pattern. If the GL location matches the angle of the null element, it will be removed from the entire pattern.

A. ELEMENT PATTERN

Fig. 2 shows the geometry of a TM_{mn} modes antenna, where the substrate is Rogers 5880 (permittivity: 2.2, loss tangent: 0.0009). For a TM_{mn} mode, the electric field of a circular ring patch antenna is given by (4)-(7) in cylindrical coordinates[22]:
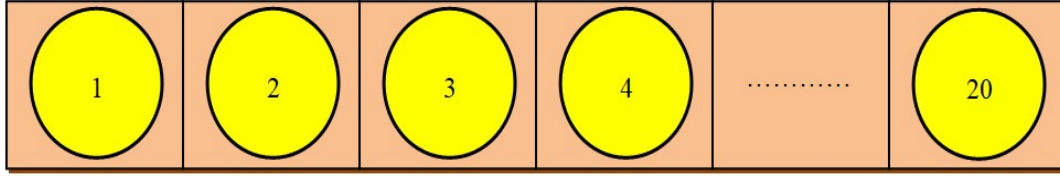
$$E_\theta^{nm} = j^n \frac{k_0 a E_0^{nm} e^{-jk_0 r}}{r} J_n(k_{mn}a) Cos(n\emptyset) F_n(\theta) \tag{4}$$

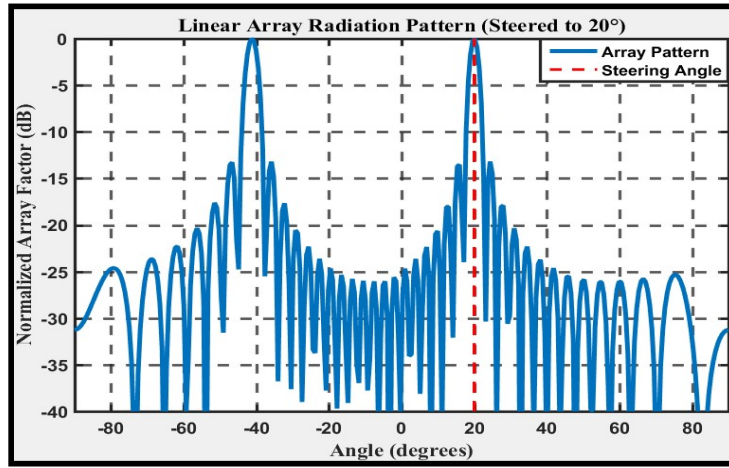$$E_\emptyset^{nm} = j^n \frac{k_0 a E_0^{mn} e^{-jk_0 r}}{r} J_n(k_{mn}a) \sin(n\emptyset) G_n(\theta) \tag{5}$$

$$F_n(\theta) = \frac{J_{n+1}(k_0 a sin\theta) + J_{n-1}(k\_0 \, a sin\theta)}{2} cos\theta \tag{6}$$

$$G_n(\theta) = \frac{J_{n+1}(k_0 a sin\theta) - J_{n-1}(k_0 a sin\theta)}{2} sin\theta \tag{7}$$

Where E_0 is the amplitude constant, and F_{mn} is the high-order mode resonance frequency, and X'_{mn} is the nth root of the derivative of the bessel function of order m. First few zeros of $J'n(x)$ are
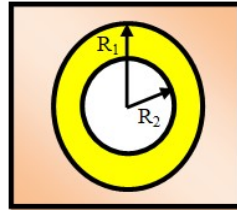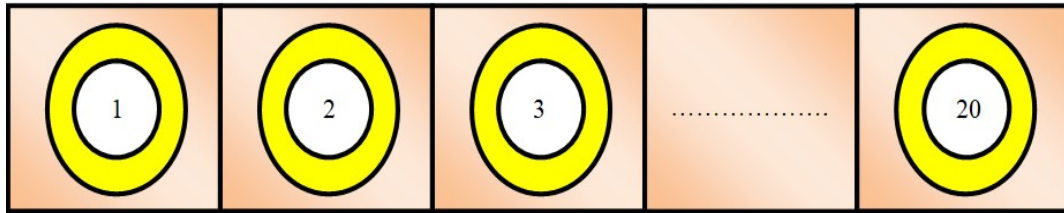
(a)

(b)

Fig. 1. (a) Geometry of a 20-element linear antenna array with element spacing of d= λo,(b) appearance of the GL in the pattern

(a)

(b)

Fig. 2. (a) Geometry of a circular slot antenna (b) array with element spacing of d= λo

listed in the Table 1. The resonant frequency is given by (8):

$$f_{mn} = \frac{X_{mn} \times c}{2\pi R\sqrt{\varepsilon_r}} \tag{8}$$

Due to the functional linearity, we can calculate the fields for each mode separately and then collect them. Fig. 3 is the normalized radiation patterns of the TM_{11} and TM_{21} modes in a ring
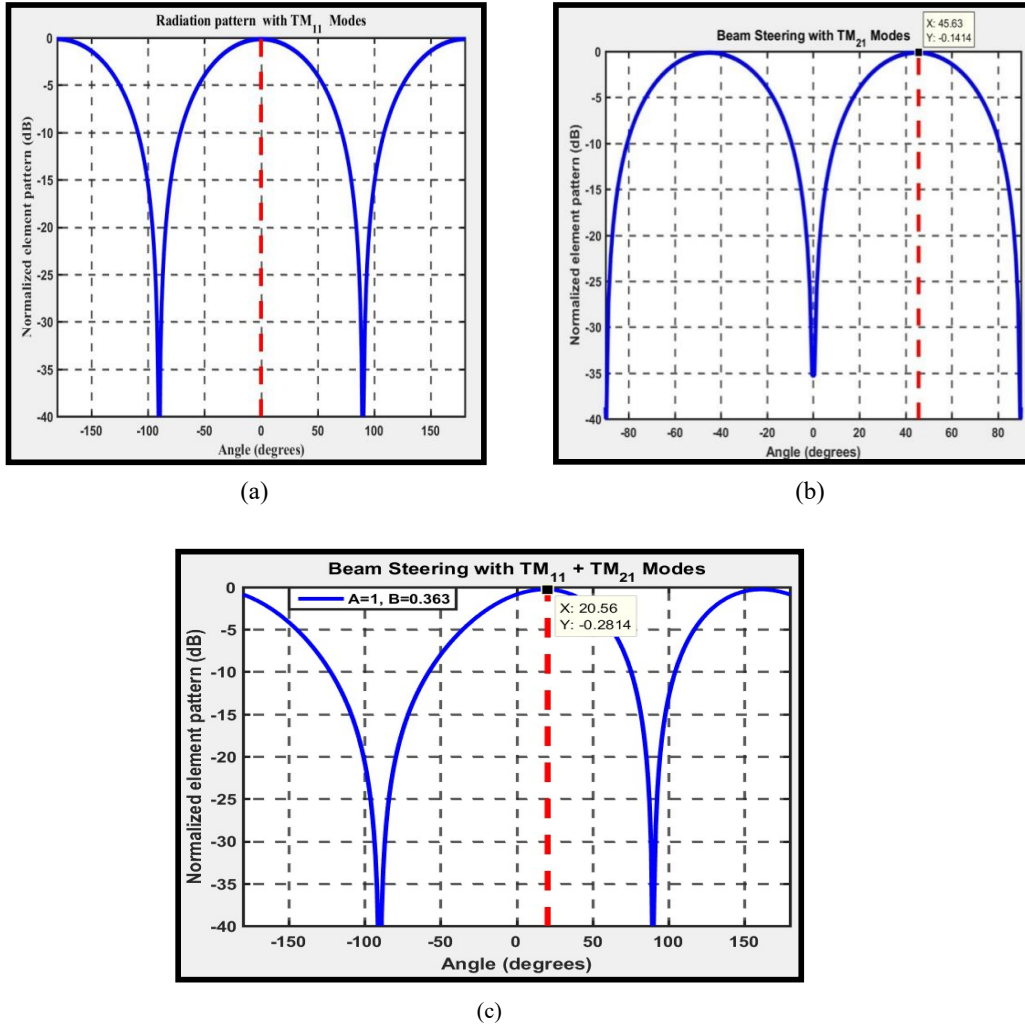
(a)

(b)

(c)

Fig. 3. Normalized radiation patterns (a) TM_{11} (b) TM_{21} (c) combined TM_{11} and TM_{21}

Table 1. First zeros of the derivatives of Bessel function ($J_{mn}'(X)$)

f_0=10GHz	TM_{11}	TM_{21}	TM_{31}
X'_{n1}	1.8412	3.0542	4.2012
R	$0.29\lambda_d$	$0.48\lambda_d$	$0.66\lambda_d$

microstrip patch antenna. By designing the antenna in a higher-order mode, we have a steering beam in the pattern. With combined TM_{11} and TM_{21} modes in Fig. 3(c), the beam of the ring antenna steers at 20.56°.

B. STEERING ELEMENT PATTERN

The advantage of high-order mode excitation is its ability to steer the beam through synthesis of phase and amplitude, and one of the important methods for appearing conical patterns is the use of
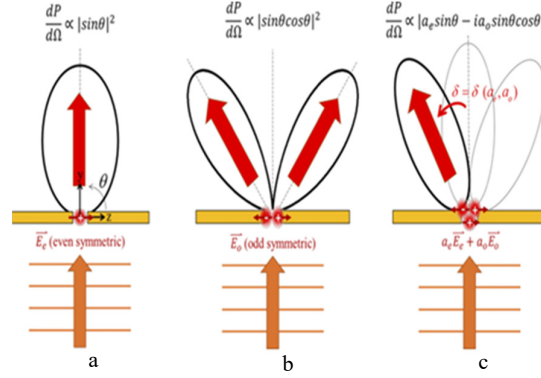
Fig. 4. radiation patterns of (a) the even mode, (b) the odd mode, and (c) the mixed mode of an antenna

this method. In other words, by exciting two orthogonal modes simultaneously with a controlled phase difference, the resulting radiation pattern can be steered. In (9) and (10), The total electric field is the sum of the first- and second-order mode fields, with the amplitude and phase of each mode relative to determining the scan angle.

$$E_\theta^{total} = E_\theta^{11} + E_\theta^{21} = A_{11}J_1(\frac{X_{11}}{a}\rho)E_0^{11}cos\emptyset F_1(\theta) + A_{21}J_2\left(\frac{X_{21}}{a}\rho\right)E_0^{21}F_2(\theta)\cos(2\emptyset + \Delta\emptyset) \quad (9)$$

$$F(\emptyset) = Acos(\emptyset) + bcos(\emptyset + 90) = Acos(\emptyset) - Bsin(2\emptyset) = (A - 2Bsin(\emptyset))\cos(\emptyset) \quad (10)$$

$$\theta_0 = \tan^{-1}(\frac{B}{A}) \quad (11)$$

The critical parameters, amplitude ratio and phase difference, affect beam steering in the equ. (11). If the phase difference, the angle between two modes, equals 90°, a traveling wave component can propagate inside the cavity. This traveling wave then rotates the asymmetrical field distribution generated by the TM_{21} mode. By electronically adjusting $\Delta\phi$ (for example, using a phase shifter), you can cause this field distribution to rotate, steering the beam in azimuth. for probing this subject, TM_{11} has maxima at ϕ=0 and ϕ=180 and TM_{21} has maxima at ϕ=0, ϕ=90, ϕ=180, and ϕ=270. When we combine two modes with $\Delta\phi$=90, the azimuthal part of the total field. by the amplitude ratio B/A, the steering angle θ_0 (elevation) is determined. The pattern of the TM_{11} mode effects in cos(ϕ), and the term (A−2Bsin(ϕ)) creates an asymmetry by weakening the field on one side (sin(ϕ)>0) and strengthening it on the opposite side (sin(ϕ)<0), therefore steering the main lobe away from broadside.

C. CONTROLLING THE BEAM USING THE RATIO OF THE AMPLITUDE MODE

A new method, using a combination of two modes through eqs. (12)-(14), allows us to change the radiation direction of an antenna. As shown in Fig. 4, the radiation direction can be changed

Fig. 5. Geometry of the element antenna (a) side view (b) top view

by combining two types of symmetrical modes (even and odd) [23].

$$E_e^f = -\frac{Z_0}{4\pi}k^2(\hat{r} \times d)\frac{e^{jkr}}{r} = \frac{-Z_0}{4\pi}k^2\frac{\alpha E_e e^{jkr}}{r}(\sin\theta\sin\emptyset\ \hat{x} - \sin\theta\cos\emptyset\ \hat{y}) \tag{12}$$

$$E_o^f = C_0\frac{E_0}{2}\frac{e^{jkr}}{r}\left[\left(-2i\sin\theta\sin\emptyset\sin\left(\frac{L}{2}cos\theta\right)\right) + \left(-2i\sin\theta\cos\emptyset\sin\left(\frac{L}{2}cos\theta\right)\right)\right] \tag{13}$$

$$E_T^f = E_e^f + E_o^f = \tag{14}$$
$$\left(-\frac{kl}{2}E_o\sin\theta\cos\theta\sin\emptyset e^{i\Delta} + E_e\sin\theta\sin\emptyset\right)c_0\frac{e^{jk_0r}}{r}\hat{x} + (i\frac{kl}{2}E_o\sin\theta\sin\theta\cos\emptyset e^{i\Delta}$$
$$- E_0\sin\theta\cos\emptyset)c_0\frac{e^{jk_0r}}{r}\hat{y}$$

$$\Gamma = \frac{dP}{d\Omega} = |a_e\sin\theta - ia_0\sin\theta\cos\theta|^2.a_0 = \frac{kL}{2}E_0e^{i\Delta}.a_e = E_0 \tag{15}$$

If $\frac{d\Gamma}{d\Omega} = 0$

$$\theta = i\frac{a_o}{a_e} \tag{16}$$

According to the relationship (15) of average radiated power per unit solid angle, $\Gamma = dP/d\Omega$, when these two antenna radiation modes are combined in one antenna, the radiated power per unit solid angle changes according to equ. (16). Where a_e and a_o are complex numbers that indicate how much the even and odd symmetric modes are combined in the antenna. Therefore, if the phase difference between the two modes is 90 degrees, the direction of radiation can be controlled, and the radiation angle is determined by changing the amplitude of the two modes. As shown in Fig. 5, the proposed antenna is dual-mode. Therefore, each mode is excited by a coaxial cable, so the antenna element has two feeds.

D. EFFECT OF HIGH ORDER MODE ON CURRENT SURFACE ANTENNA

Utilizing the high-order mode antenna to enhance antenna performance affects the surface current distribution. When an antenna is designed for a higher-order mode, the electrical length of the antenna increases. For example, higher-order mode patch antennas suggest high gain due to their increased size. The appearance of the S_{LL} in the radiation pattern and its reduction are important. Therefore, one of the important problems in higher-order mode antennas is the appearance of the

S_{LL}. The current distribution is divided into three parts. In other words, we have two regions, in phase and out of phase, on the surface of the antenna in Fig. 6. Currents in out-of-phase have an opposite direction to in-phase currents. Thus, we have a null at 0° in the radiation pattern.

IV. SYNTHESIS NULL IN SUBARRAY PATTERN

As mentioned, a subarray is a group of antenna elements that includes elements within it. Therefore, they are controlled together as a single unit, rather than independently. The synthesis of a subarray antenna, which involves meeting specific requirements such as low SLLs and beam steering, consists of designing elements grouped into subarrays for the synthesis pattern antenna.

A. ARRAY FACTOR FORMULATION

The equ. (17) array factor of a subarray antenna is a multiple of the subarray factor $S_S(\theta,\phi)$ and the full array factor $S_F(\theta,\phi)$. Suppose that the structure of the array consists of M subarrays and N elements per subarray, then the subarray factor is given by (18-19):

$$AF(\theta,\emptyset) = S_F(\theta,\emptyset) \times S_S(\theta,\emptyset) \tag{17}$$

$$AF(\theta,\emptyset) = \sum_{m=1}^{M} W_m \left(\sum_{n=1}^{N} a_n e^{jk\hat{r}.d_n} \right) e^{jk\hat{R}.D_m} \tag{18}$$

For a linear array along the x-axis with non-uniform subarrays:

$$AF(\theta,\emptyset) = \sum_{m=1}^{M} W_m e^{jk(n-1)D_x sin\theta} \left(\sum_{n=1}^{N} a_n e^{jk(m-1)d_x sin\theta} \right) \tag{19}$$

Where W_n, a_n, D_X, and d_x are complex weights for the subarray, excitation for the full array, subarray spacing, and spacing between every element within the subarray. For transmitting this formulation to a matrix, it provides a rigorous mathematical framework for synthesizing the radiation pattern of a subarray antenna.

B. MATRIX FORMULATION FOR SUBARRAY ANTENNA SYNTHESIS

Assume the linear subarray model is shown in Fig. 7(a) The antenna array is composed of M subarrays, and there are four elements in every unit subarray. For the N element in the M subarray, the phase delay is given by (20):

$$Phase\ delay = e^{jk\hat{r}(R_m+r_n)} \tag{20}$$

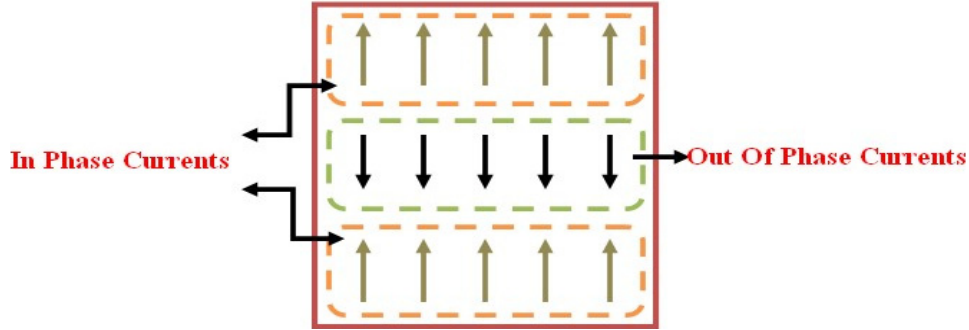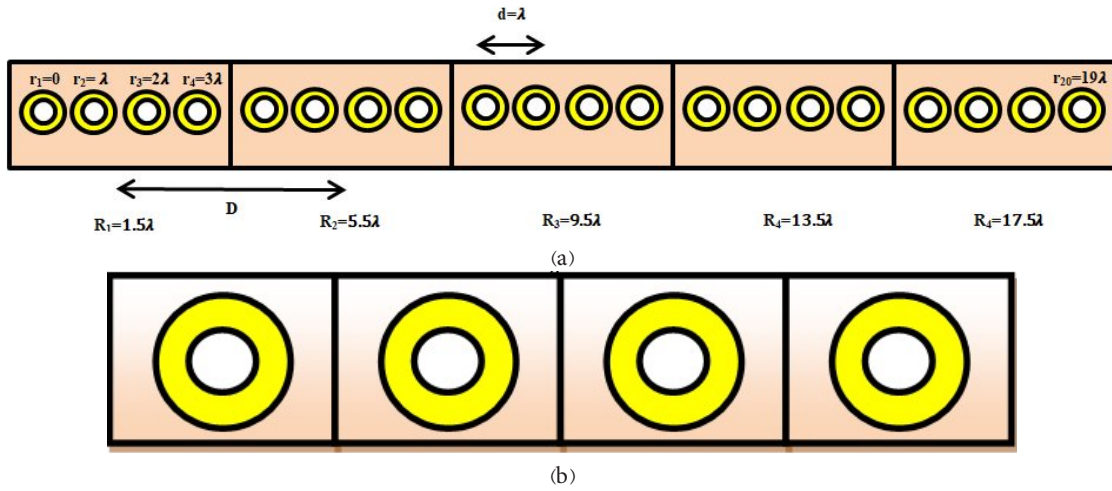Therefore, the matrix formulations (21)-(23) are a weighted sum of subarray responses in the model shown in Fig. 7.

Fig. 6. Surface currents of patch antenna operating in TM$_{mn}$ mode

(a)

(b)

Fig. 7. (a) Linear M subarray antenna, (b) elements within every subarray

$$S_m(\theta,\emptyset) = [e^{jk\hat{r}(R_m+r_1)}, e^{jk\hat{r}(R_m+r_2)}, e^{jk\hat{r}(R_m+r_3)} \dots.. e^{jk\hat{r}(R_m+r_N)}]^T \in C^N \tag{21}$$

$$V_m(\theta,\emptyset) = [e^{jk\hat{r}(R_1)}, e^{jk\hat{r}(R_2)}, e^{jk\hat{r}(R_3)} \dots.. e^{jk\hat{r}(R_M)}]^T \in C^M \tag{22}$$

$$AF = [W_1, W_2, \dots\dots, W_M] \times \begin{bmatrix} S_{11} & S_{1N} \\ S_{M1} & S_{NM} \end{bmatrix} \times [a_1, a_2, \dots\dots, a_N]^T \tag{23}$$

In Fig. 8 the radiation pattern of a subarray antenna with M subarrays and N inter-elements within every subarray is shown. The excitation ratio and phase shift controls beam scan angle and null position. With the scanning main beam at 20° in Fig. 8 (a), we can see the appearance of the GL at -40°. To achieve GL reduction in the radiation pattern, the scanning pattern in the subarray factor and element must match. When the circular ring patch antenna is excited in a higher-order mode, it can scan the beam. As mentioned, adding null to the radiation pattern allows us to omit the GL. In other words, the secondary major lobe appears around θ_o = -40°. As a result, steering the null in the radiation pattern at -40° removes the GL in the total radiation pattern. As shown in Fig. 8, the radiation pattern of the proposed subarray antenna reduced GLs. By

utilizing the self-scanning and Optimization, the GL is reduced below -21.54 dB using dual-mode. Therefore, excitation ratio selection at the element level controls beam tilt and nulls. Optimizing the amplitudes of the subarrays (while maintaining the phase for beam steering) is a common method to achieve low SLLs. Least squares optimization finds the best curve fit to your data by minimizing the sum of squares of the difference between the observed and predicted values. For example, assume a scatterplot of points is drawn, and a straight line is drawn through the middle of these points. This line is where the sum of the squares' areas drawn from the points to the line is the smallest possible value. If the fitted line follows the equation (24):

$$y = \beta_0 + \beta_1 x_1 + \beta_2 x_2 + \cdots \beta_n x_n \tag{24}$$

In (25) matrix form equation for extracted variable of x too:

$$Ax = b \tag{25}$$

A is a $m \times n$ matrix, b is a $m \times 1$ vector of the observed outcomes, and x is a $n \times 1$ vector of the unknown parameters. the β coefficients are determined by solved this equation. The goal is to find the vector x, equs. (26)-(28), that minimizes the sum of squared residuals:

$$\min_x |Ax - b| \tag{26}$$

Equation (27) is the solution for the parameter vector x, Where x is our best estimate for the parameters.

$$x = (A^T A)^{-1} A^T b \tag{27}$$

Because the magnitude of the S_{LL} is not valuable for Fig. 8(b), the goal is to find the complex weights for elements a_n and subarrays w_m that produce a radiation pattern $AF(\theta,\varphi)$ as close as possible to a desired pattern $F_{desired}(\theta,\varphi)$. Choosing the effective weight means combining the weights for the subarray and element. We can achieve a better amplitude for the structure. Through the method of the least-squares optimization[24], we can minimize the squared error between the synthesized pattern and the desired pattern. We often need to control sidelobes.

$$\min_X \|Ax - F_{disired}\|^2 \tag{28}$$

The basic cost function is through of equal (29) the Mean Squared Error (MSE) between the synthesized and desired patterns:

$$J(w, a) = \sum_{k=1}^{K} |AF(\theta_k, \emptyset_k) - F_{desired}(\theta_k, \emptyset_k)|^2 \tag{29}$$

Expanded Form in equatin (30):

$$J(w, a) = \sum_{k=1}^{K} \left| \sum_{m=1}^{M} w_m \left(\sum_{n=1}^{N} a_n e^{jk\,\hat{r}_k \cdot (R_m + r_m)} \right) - F_{desired}(\theta_k, \emptyset_k) \right|^2 \tag{30}$$
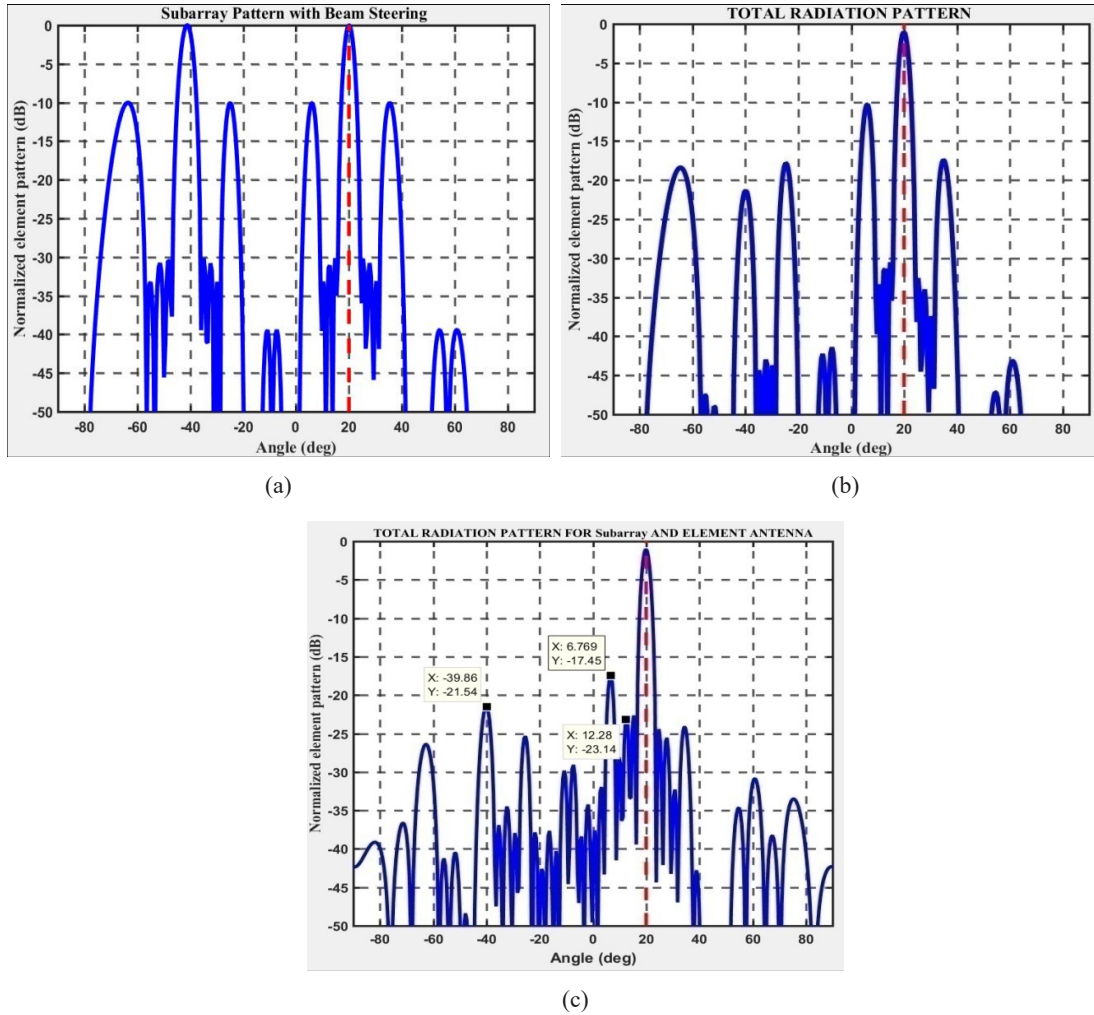
(a)

(b)

(c)

Fig. 8. Normalize radiation pattern

a) subarray antenna b) total pattern c) optimization amplitude total pattern

Table 2. Comparison of proposed antenna with other works

Ref	GL
[11]	-16.2dB
[12]	-17dB
[13]	-20dB
[14]	-22dB
[20]	-20dB
[7]	-16dB
This-work	-21.54dB

As shown in Fig. 8(c), the magnitude of the GL and S_{LL} has been reduced by amplitude optimization. The value of the GL at -40° decreases to -21.54dB, and S_{LL}. The pattern with

the subarray also improves sidelobes by -23.14 dB. Finally, Table 2 presents the results of the proposed antenna and compares them with other references in terms of the GL. It can be seen that the proposed subarray antenna is better than the antennas in the references.

V. CONCLUSION

Subarrays are a group of elements within an array that are useful for improving the performance of an antenna. The main advantages of this technique are reduced complexity, Cost Efficiency, and system flexibility. This research presents GL reduction for non-uniform linear subarrays using high-order modes. Due to the GL, the undesirable lobes are in the visible region of the antenna, so the main idea for suppressing them is to add a null at the GL angle, which decreases the magnitude of the GL. GL occurs when the element spacing in an antenna exceeds a specific limit compared to the wavelength of the signal. An important method for reducing grating lobes includes the generation of nulls in the radiating pattern. As a result, the use of the characteristic mode method in controlling the distribution of multiple currents in the higher-order mode is found to be very effective in steering the radiation pattern. The proposed technique exhibits a simulated reduction in the Grating lobe level by -21.54 dB.

REFERENCES

[1] F. Boulos, S. Caizzone, and A. Winterstein, "a Subarray-Based Antenna Design for Satellite Communications Ground Terminals in Ka Band," *Ka Broadband Commun. Conf.*, vol. 2021–Sept. 2021.

[2] Tony Azar, "Overlapped Subarrays: Review and Update," *IEEE Antennas Propag. Mag.*, vol. 55, no. 2, 2013.

[3] T. Jeong, J. Yun, K. Oh, J. Kim, D. Woongwoo, and K. Cheol Hwang, "Shape and weighting optimization of a subarray for an mm-wave phased array Antenna," *Appl. Sci.*, vol. 11, no. 15, 2021.

[4] R. L. Haupt, "Optimized weighting of uniform subarrays of unequal sizes," *IEEE Trans. Antennas Propag.*, vol. 55, no. 4, pp. 1207–1210, 2007.

[5] Z. Wu, P. Wu, W. Liu, and Z. Zhang, "Adaptive Subarray Partitioning for Large-Scale Phased Arrays Using ISODATA," *Electron. Lett.*, vol. 61, no. 1, 2025.

[6] E. Kim, I. Kim, and W. Kim, "Non-Uniform MIMO Array Design for Radar Systems Using Multi-Channel Transceivers," *Remote Sens.*, vol. 15, no. 1, 2023.

[7] J. Sun, K. Zhang, J. Ye, X. Wu, and G. Hua, "A Novel Design of Non-Uniform Limited Scan Array Based on Tri-Polarized Metamaterial Element," *IEEE Access*, vol. 13, pp. 126574–126581, 2025.

[8] S. Jebali, H. Keshavarz "Performance of Target Detection in Phased-MIMO Radars," Journal of Communication Engineering, Vol. 7, No. 2, 2018.

[9] C. Liu, J. Wang, W. Cui, H. Xu, and B. Yang, "A signal separation method based on the subarray beam synthesis," *IET Radar, Sonar Navig.*, vol. 17, no. 2, pp. 191–199, 2023.

[10] H. Zhao, H. Chu, X. Zhu, and Y. Guo, "A Subarray-based Approach for Gain Flatness Improvement of Multibeam Antennas," *IEEE Reg. 10 Annu. Int. Conf. Proceedings/TENCON*, vol. 2022–November, 2022.

Journal of Communication Engineering (JCE)

Etebarian Khorasgani & Ghorbani | Grating-Lobe Reduction for Non-Uniform Linear ...

[11] L. Yang, K. Wang, and H. Sun, "A grating lobe suppression method for displaced subarrays using genetic algorithm," *IET Microwaves, Antennas Propag.*, vol. 16, no. 7, pp. 457–464, 2022.

[12] M. Boyarsky, M. F. Imani, and D. R. Smith, "Grating lobe suppression in metasurface antenna arrays with a waveguide feed layer," *Opt. Express*, vol. 28, no. 16, p. 23991, 2020.

[13] H. Wang, D. G. Fang, and Y. L. Chow, "Grating lobe reduction in a phased array of limited scanning," *IEEE Trans. Antennas Propag.*, vol. 56, no. 6, pp. 1581–1586, 2008..

[14] Y. Zhang, W. Cao, Z. Qian, S. Shi, and W. Peng, "Low Grating Lobe Array Antenna with Electrically Large Property Based on TM50 Mode," *IEEE Access*, vol. 7, pp. 32897–32906, 2019.

[15] Z. Iqbal and M. Pour, "Grating Lobe Mitigation in Scanning Planar Phased Array Antennas," *IEEE Int. Symp. Phased Array Syst. Technol.*, vol. 2019–October, 2019.

[16] B. R. S. Reddy and D. Vakula, "Grating Lobe Suppression with Element Count Optimization in Planar Antenna Array," *J. Electromagn. Anal. Appl.*, vol. 7, no. 2, pp. 31–40, 2015.

[17] X. P. Li, M. M. Li, J. F. Ji, Q. Q. Sun, W. Li, and A. X. Zhang, "A Dual-Band Low-Profile Microstrip Antenna with Fan-Shaped and Rectangular Beams," *Electron.*, vol. 12, no. 19, 2023.

[18] Z. Iqbal and M. Pour, "Exploiting Higher Order Modes for Grating Lobe Reduction in Scanning Phased Array Antennas," *IEEE Trans. Antennas Propag.*, vol. 67, no. 11, pp. 7144–7149, 2019.

[19] J. Anguera, A. Andujar, and J. Jayasinghe "High Directivity Microstrip Patch Antennas based on TModd-0 modes," IEEE Antennas and Wireless Propagation Letters., vol. 19, pp. 38-43, 2019.

[20] Z. Ahmed, A. Muhammad, and M. Bin Ihsan, "Improving the Sidelobe Level, Return Loss and Bandwidth of Notch-Loaded TM30Mode Patch via Fractal-Slot," *IEEE Access*, vol. 10, pp. 19917–19924, 2022.

[21] C.A. Balanis, " Modern antenna handbook " .John Wiley & Sons,2012.

[22] W. L. Stutzman and G. A. Thiele "Antenna theory and design". John Wiley & Sons, 2012

[23] H.-M. Kim and M.-K. Kim, "Beam steering of a single nanoantenna," *Opt. Express*, vol. 28, no. 11, p. 16822, 2020.

[24] J. M. F. ten Berge, "Least Squares Optimization in Multivariate Analysis," *Leiden Univ.*, vol. 34, p. 96, 2005.